Fundamental Analysis of an Electrohydraulic Servomechanism Operated by PWM Mode

By

Taizo SAWAMURA*, Hideo HANAFUSA† and Takashi INUI‡

(Received October 31, 1959)

When an electrohydraulic servomechanism is used as a high performance servo, the PWM mode is interesting for the reduction of required accuracy in manufacturing valves and for removing the effects such as frictions of various parts. The manufactured servomechanism is composed of a torquemotor, a flapper-nozzle, a spool valve and an actuator. The input current to the torquemotor is in the form of a pulse-width-modulated wave supplied by a multivibrator, and the displacements of the flapper and the spool are restricted by the stoppers.

The forces acting on the flapper caused by jets from nozzles are analyzed, and it is shown that the forces become as small as negligible, and sometimes accelerate the the flapper movement with a proper choice of discharge coefficient of nozzle. This means that the flapper-nozzle is favorable for a preamplifier in the PWM mode operation. As the results of the analysis, the displacement of the spool is approximately in the form of a trapezoidal pulse with certain time lag for the input to the torquemotor. When the load of the actuator consists of a mass and friction, the dither amplitude of the actuator piston is obtained exactly for the trapezoidal pulse input. The pulse period is determined by the waveshape of the spool displacement and the dither amplitude of the actuator piston. The analytical results were verified by experiments.

1. Introduction

There are two principal difficulties in designing a high performance hydraulic servomechanism. One is the extremely small tolerance allowed for the metering orifice of the spool valve, and the other is the inherent nonlinearities of the hydraulic elements. One of the operating methods of electro-hydraulic servomechanism is the PWM mode operation in which the input signal to a spool valve is given in the form of pulse-width-modulated waves. This PWM operation reduces the accuracy required for hydraulic equipments and removes the effects of nonlinearities such as frictions in mechanical parts[1]. This operation is effective for high power or high temperature servos[2], and for preventing stick motions in very low-speed servos.

* Automation Research Laboratory
† Faculty of Industrial Arts, Kyoto Technical University
‡ Department of Aeronautical Engineering

The electrohydraulic servomechanism composed of a torquemotor, a flapper-nozzle, a spool valve and an actuator, was built. The fundamental characteristics of these elements are analyzed for the PWM mode operation. The pulse period is restricted by the characteristics of hydraulic parts and the criterion is obtained to determine the period of pulse.

2. Construction of an Experimental Apparatus

The experimental apparatus is consisted of a multivibrator, a torquemotor, a flapper-nozzle, a spool valve and an actuator. The schematic diagram of the hydraulic equipment is shown in Fig. 1. The output displacement of the actuator

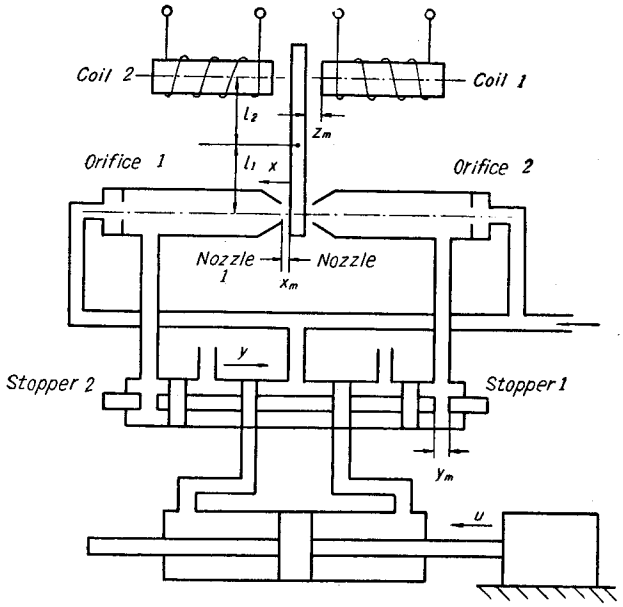

Fig. 1. Schematic diagram of an experimental apparatus.

is sensed by a differential transformer the output of which is used for the feedback of the servo loop and for the record of the output. Waveshapes of rectangular pulses excited by the multivibrator are shown in Fig. 2 (a) for no signals, and (b) for signals. Rectangular pulses are fed to power amplifiers, and the plus or minus current in Fig. 2 is given to Coil 1 or Coil 2 alternately, and drives the flapper. When the flapper passes the neutral position, the spool begins to move. After the flapper closes one of the nozzles, the spool moves at a constant velocity and is stopped by a stopper. Untill the spool arrives at the neutral position, the actuator piston

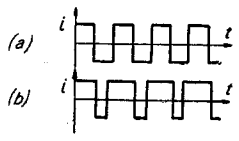

Fig. 2. Waveshapes of PWM mode.

continues the motion in the same direction, but moves adversely after the spool passes the neutral position. The actuator piston moves gradually in the desired direction while making such small oscillations.

3. Flow characteristics of a flapper-nozzle

In the flapper-nozzle mechanism shown in Fig. 1, the flow rates are related to the pressures as follows:

$$Q_{01} = \alpha_0 A_0 \sqrt{\frac{2}{\rho}(p_s - p_{01})} , \tag{1}$$

$$Q_{02} = \alpha_0 A_0 \sqrt{\frac{2}{\rho}(p_s - p_{02})} , \tag{2}$$

$$Q_{n1} = \alpha_n A_n \sqrt{\frac{2}{\rho}(p_{01} - p_{n1})} , \tag{3}$$

$$Q_{n2} = \alpha_n A_n \sqrt{\frac{2}{\rho}(p_{02} - p_{n2})} , \tag{4}$$

$$Q_{n1} = \alpha_f \pi d_n (x_m - x) \sqrt{\frac{2}{\rho} p_{n1}} , \tag{5}$$

$$Q_{n2} = \alpha_f \pi d_n (x_m + x) \sqrt{\frac{2}{\rho} p_{n2}} , \tag{6}$$

$$Q_{01} = Q_{n1} + A_v \frac{dy}{dt} , \tag{7}$$

$$Q_{02} = Q_{n2} - A_v \frac{dy}{dt} . \tag{8}$$

Equating Eqs. (3) and (5),

$$p_{n1} = \frac{\alpha_n^2 A_n^2}{\alpha_n^2 A_n^2 + \alpha_f^2 \pi^2 d_n^2 (x_m - x)^2} p_{01} . \tag{9}$$

Using Eqs. (1), (3), (7) and (9),

$$\frac{p_{01}}{p_s} = \frac{(-w_1 w_3 + \sqrt{1 + w_1^2 - w_3^2})^2}{(1 + w_1^2)^2} , \tag{10}$$

where

$$w_1 = \frac{\alpha_n A_n}{\alpha_0 A_0} \cdot \frac{\alpha_f \pi d_n (x_m - x)}{\sqrt{\alpha_n^2 A_n^2 + \alpha_f^2 \pi^2 d_n^2 (x_m - x)^2}} , \tag{11}$$

$$w_3 = \frac{A_v}{\alpha_0 A_0} \sqrt{\frac{\rho}{2 p_s}} \left(\frac{dy}{dt} \right) . \tag{12}$$

Using Eqs. (2), (4), (6) and (8),

$$p_{n2} = \frac{\alpha_n^2 A_n^2}{\alpha_n^2 A_n^2 + \alpha_f^2 \pi^2 d_n^2 (x_m + x)^2} p_{02} , \tag{13}$$

$$\frac{p_{02}}{p_s} = \frac{(w_2 w_3 + \sqrt{1 + w_2^2 - w_3^2})^2}{(1 + w_2^2)^2} , \tag{14}$$

where

$$w_2 = \frac{\alpha_n A_n}{\alpha_0 A_0} \cdot \frac{\alpha_f \pi d_n (x_m + x)}{\sqrt{\alpha_n^2 A_n^2 + \alpha_f^2 \pi^2 d_n^2 (x_m + x)^2}} . \tag{15}$$

The results of calculation of Eqs. (10) and (14) for the experimental apparatus are shown in Fig. 3.

Using Eqs. (10) and (14), the statical flow characteristics of the flapper-nozzle are obtained as follows:

$$\frac{p_{01}}{p_s} - \frac{p_{02}}{p_s} = \frac{(-w_1 w_3 + \sqrt{1 + w_1^2 - w_3^2})^2}{(1 + w_1^2)^2} - \frac{(w_2 w_3 + \sqrt{1 + w_2^2 - w_3^2})^2}{(1 + w_2^2)^2} . \tag{16}$$

The results of calculation of the statical flow characteristics are shown in Fig. 4

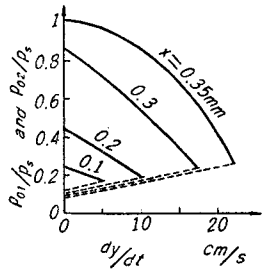

Fig. 3. Relation between displacement of a flapper, velocity of a spool and back pressure of nozzles in the flapper-nozzle.

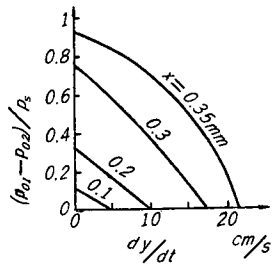

Fig. 4. Relation between displacement of a flapper, velocity of a spool and effective pressure difference in the flapper-nozzle.

4. Forces acting on a flapper

Hydraulic flow forces acting on the flapper are obtained as follows, using Eqs. (9) and (13):

$$f_{n1} = -\left(p_{n1} A_n + \rho Q_{n1} \frac{Q_{n1}}{A_n}\right) = \frac{-\alpha_n^2 A_n^2}{\alpha_n^2 A_n^2 + \alpha_f^2 \pi^2 d_n^2 (x_m - x)^2} \left\{A_n + 2\alpha_f^2 \pi^2 d_n^2 (x_m - x)^2 \frac{1}{A_n}\right\} p_{01} , \tag{17}$$

$$f_{n2} = p_{n2} A_n + \rho Q_{n2} \frac{Q_{n2}}{A_n} = \frac{\alpha_n^2 A_n^2}{\alpha_n^2 A_n^2 + \alpha_f^2 \pi^2 d_n^2 (x_m + x)^2} \left\{A_n + 2\alpha_f^2 \pi^2 d_n^2 (x_m + x)^2 \frac{1}{A_n}\right\} p_{02} . \tag{18}$$

When the spool stops at the stopper, the following relations are obtained, substituting $w_3 = 0$ in Eqs. (10) and (14):

$$p_{01} = \frac{1}{1 + w_1^2} p_s , \qquad p_{02} = \frac{1}{1 + w_2^2} p_s . \tag{19}$$

Substituting p_{01} and p_{02} in Eqs. (17) and (18), the hydraulic flow forces of Nozzle 1 and Nozzle 2 are obtained and they are denoted by f_{ns1} and f_{ns2}, respectively. The hydraulic flow force of dual nozzle, f_{ns}, is the sum of f_{ns1} and f_{ns2}, and is obtained as follows:

$$f_{ns} = f_{ns1} + f_{ns2}$$
$$= \frac{-4\alpha_0^2 A_0^2 \alpha_n^2 A_n^3 \alpha_f^2 \pi^2 d_n^2 x_m x (\alpha_0^2 A_0^2 + \alpha_n^2 A_n^2 - 2\alpha_0^2 A_0^2 \alpha_n^2) p_s}{\{\alpha_0^2 A_0^2 \alpha_n^2 A_n^2 + (\alpha_n^2 A_n^2 + \alpha_0^2 A_0^2)\alpha_f^2 \pi^2 d_n^2 (x_m - x)^2\}\{\alpha_0^2 A_0^2 \alpha_n^2 A_n^2 + (\alpha_n^2 A_n^2 + \alpha_0^2 A_0^2)\alpha_f^2 \pi^2 d_n^2 (x_m + x)^2\}} . \tag{20}$$

When the spool is moving, the following relation is obtained:

$$p_{01} = p_{02} = p_{0m} \tag{21}$$

where p_{0m} is given by the intersection of the solid curves and the dotted curves in Fig. 3. Substituting Eq. (21) in Eqs. (17) and (18), the hydraulic flow forces of Nozzle 1 and Nozzle 2 are obtained and they are denoted by f_{nm1} and f_{nm2}, respectively. The hydraulic flow force of dual nozzle, f_{nm}, is the sum of f_{nm1} and f_{nm2}, and is obtained as follows:

$$f_{nm} = f_{nm1} + f_{nm2}$$
$$= \frac{-4\alpha_n^2 A_n^3 \alpha_f^2 \pi^2 d_n^2 x_m x (1 - 2\alpha_n^2) p_{0m}}{\{\alpha_n^2 A_n^2 + \alpha_f^2 \pi^2 d_n^2 (x_m - x)^2\}\{\alpha_n^2 A_n^2 + \alpha_f^2 \pi^2 d_n^2 (x_m + x)^2\}} . \tag{22}$$

From Eq. (22), if α_n is close to 0.71, the hydraulic flow force is negligible and this is the ordinary condition for hydraulic nozzles. It is remarkable that the hydraulic flow force acts as the negative spring for $\alpha_n > 0.71$. When the torquemotor circuit is switched, f_{ns} acts on the flapper and accelerates the flapper motion. After the spool begins to move, f_{nm} acts on the flapper, but the influence of f_{nm} is usually negligible. Therefore, we may consider only the torquemotor force acting on the flapper in analyzing the motion of the flapper.

5. Motions of a flapper and a spool

The equation of motion of the flapper after the electric current is switched from Coil 2 to Coil 1 can be written as

$$\frac{I_f}{l_1 l_2} \frac{d^2x}{dt^2} = \frac{K_m i_1^2 n^2}{\{z_m - (l_2/l_1)x\}^2} . \tag{23}$$

Using the initial condition of $x = -x_m$ and $(dx/dt) = 0$ at $t = 0$, Eq. (23) can be integrated as follows:

$$t = \sqrt{\frac{I_f l_2}{2K_m i_1^2 n^2 l_1^3}\left(\frac{l_1}{l_2} z_m + x_m\right)}\left[\sqrt{(x + x_m)\left(\frac{l_1}{l_2} z_m - x\right)} + \left(\frac{l_1}{l_2} z_m + x_m\right) \sin^{-1}\sqrt{\frac{x + x_m}{(l_1/l_2) z_m + x_m}}\right] . \tag{24}$$

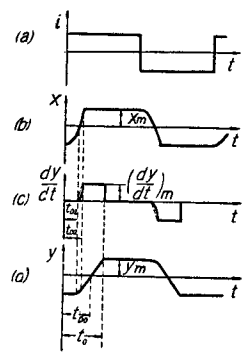

Fig. 5. Waveshapes of electric current in a torquemotor, displacement of a flapper, velocity of a spool and displacement of a spool.

The electric current and the displacement of the flapper are shown in Fig. 5 (a) and (b), respectively. t_{D1} is obtained by substituting $x = 0$ in Eq. (24) and t_{D2} by substituting $x = x_m$.

When the electric current is switched to Coil 1, the

spool stands still at Stopper 2 untill the flapper arrives at the neutral position. After the flapper passes through the neutral position, the spool moves with velocity corresponding to the flapper position. The spool velocity is obtained by the relation of x and (dy/dt) on the abscissa in Fig. 4. After the flapper closes Nozzle 1, the spool moves with a constant velocity, $(dy/dt)_m$, till it stops at Stopper 1. When the spool stops at the stopper, the back pressure of Nozzle 1, p_{01}, rises abruptly and pushes the flapper to the neutral position. The torque-motor force should be sufficient to overcome the flow force at the moment.

The velocity of the spool is shown in Fig. 5 (c), and approximated by the dotted line. The approximated velocity is as follows:

$$\left.\begin{aligned} \frac{dy}{dt} &= 0 : \quad 0 < t < t_{D1} \\ \frac{dy}{dt} &= \frac{t-t_{D1}}{t_{D2}-t_{D1}}\left(\frac{dy}{dt}\right)_m : \quad t_{D1} < t < t_{D2} \\ \frac{dy}{dt} &= \left(\frac{dy}{dt}\right)_m : \quad t_{D2} < t < t_D \end{aligned}\right\}, \tag{25}$$

The maximum velocity, $(dy/dt)_m$, is obtained as follows by substituting $p_{01}=p_{02}$ and $x=x_m$ in Eq. (16).

$$\left(\frac{dy}{dt}\right)_m = \frac{1}{A_v}\sqrt{\frac{2p_s}{\rho}}\frac{\alpha_0 A_0 \alpha_n A_n \alpha_f \pi d_n x_m}{\sqrt{\alpha_0^2 A_0^2 \alpha_n^2 A_n^2 + 4\alpha_0^2 A_0^2 \alpha_f^2 \pi^2 d_n^2 x_m^2 + \alpha_n^2 A_n^2 \alpha_f^2 \pi^2 d_n^2 x_m^2}}. \tag{26}$$

The displacement of the spool is shown in Fig. 5 (d). t_{D0} and t_D are obtained as follows, using the approximation of the spool velocity:

$$t_{D0} = \frac{1}{2}(t_{D1}+t_{D2}) + \frac{y_m}{(dy/dt)_m}, \tag{27}$$

$$t_D = \frac{1}{2}(t_{D1}+t_{D2}) + \frac{2y_m}{(dy/dt)_m}. \tag{28}$$

6. Motion of an Actuator Piston

It is assumed that the load of the actuator consists only of a mass M_l and Coulomb friction F_l, and that the oil compressibility is negligible. The displacement of the spool is shown in Fig. 5 (d), and is approximated by a trapezoidal pulse in Fig. 6, where $\tau_s=2y_m/(dy/dt)_m$. When $y>0$, the following equation is obtained for the spool valve:

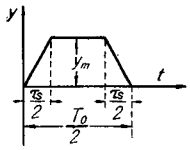

Fig. 6. Approximated trapezoidal pulse.

$$v = \frac{K_q}{\sqrt{2}}\frac{y}{A_a}\sqrt{p_s - \frac{F_l}{A_a} - \frac{M_l}{A_a}\frac{dv}{dt}} \tag{29}$$

Eq. (29) can be integrated as follows for each straight range in Fig. 6.

1) $0<t<(\tau_s/2)$

Substitution of $y=2y_m t/\tau_s$ makes Eq. (29)

$$\frac{dv}{dt}=\frac{A_a}{M_l}\left(p_s-\frac{F_l}{A_a}\right)-\frac{1}{2}\left(\frac{A_a\tau_s}{K_q y_m}\right)^2\frac{A_a}{M_l}\left(\frac{v}{t}\right)^2. \tag{30}$$

This homogeneous equation can be transformed as follows by substituting $v=tz$.

$$\left.\begin{aligned} z+t\frac{dz}{dt}&=f(z),\\ f(z)&=\frac{A_a}{M_l}\left(p_s-\frac{F_l}{A_a}\right)-\frac{1}{2}\left(\frac{A_a\tau_s}{K_q y_m}\right)^2\frac{A_a}{M_l}z^2. \end{aligned}\right\} \tag{31}$$

Eq. (31) has two types of the solutions.

(a) In Case of $(dz/dt)=0$

In this case the solution of Eq. (31) is:

$$z=\frac{v}{t}=\frac{a-b}{h}\quad\text{and}\quad\frac{-(a+b)}{h}, \tag{32}$$

where

$$a=\sqrt{2\left(p_s-\frac{F_l}{A_a}\right)\left(\frac{A_a\tau_s}{K_q y_m}\right)^2+\left(\frac{M_l}{A_a}\right)^2},\qquad b=\frac{M_l}{A_a},\qquad h=\left(\frac{A_a\tau_s}{K_q y_m}\right)^2. \tag{33}$$

(b) In Case of $(dz/dt)\neq 0$

In this case, the result of the integration of Eq. (31) becomes as follows, using representations of Eq. (33):

$$v=\frac{-t}{h}\cdot\frac{(a+b)-(a-b)C_1 t^{a/b}}{1+C_1 t^{a/b}}, \tag{34}$$

where C_1 is an integral constant, and is determined by the initial condition of $v=v_0$ at $t=t_0$. It is

$$C_1=\left[t^{-a/b}\left\{\frac{(a+b)t+hv}{(a-b)t-hv}\right\}\right]_{t=t_0,\,v=v_0}. \tag{35}$$

Eqs. (32) and (34) represent a group of curves as shown in Fig. 7. When the valve port is opening, only the thick line in Fig. 7 has the physical meaning.

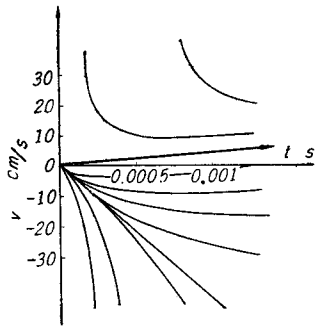

Fig. 7. Velocity of an actuator piston in opening the valve port.

2) $(\tau_s/2)<t<(T_0-\tau_s)/2$

Substitution of $y=y_m$ makes Eq. (29)

$$\frac{dv}{dt}=\frac{A_a}{M_l}\left(p_s-\frac{F_l}{A_a}-2\frac{A_a^2v^2}{K_q^2y_m^2}\right). \tag{36}$$

Eq. (36) can be directly integrated as follows:

$$v=\frac{K_q y_m}{\sqrt{2}\,A_a}\sqrt{p_s-\frac{F_l}{A_a}}\tanh\left\{\frac{\sqrt{2}\,A_a^2}{K_q y_m M_l}\sqrt{p_s-\frac{F_l}{A_a}}\,(t+C_2)\right\}. \tag{37}$$

C_2 is an integral constant, and is determined by the initial condition of $v=v_0$ at $t=0$, where the origin of time is taken at $t=\tau_s/2$.

$$C_2 = \frac{K_q y_m M_l}{A_a^2\sqrt{2}\{p_s-(F_l/A_a)\}} \tanh^{-1}\left\{\frac{\sqrt{2}A_a v_0}{K_q y_m\sqrt{p_s-(F_l/A_a)}}\right\}. \tag{38}$$

The displacement of the actuator piston, u, is obtained by integrating Eq. (37) and using an initial condition of $u=u_0$ at $t=0$.

$$u = \frac{K_q^2 y_m M_l}{2A_a^3} \log\cosh\left\{\frac{\sqrt{2}A_a^2}{K_q M_l y_m}\sqrt{p_s-(F_l/A_a)}(t+C_2)\right\}+u_0. \tag{39}$$

3) $(T_0-\tau_s)/2<t<(T_0/2)$

If the origin of time is taken at $t=(T_0-\tau_s)/2$, the spool displacement becomes as $y=y_m-(2y_m t/\tau_s)$. By substituting $y=y_m-(2y_m t/\tau_s)$ and replacing t by

$$t_1 = (\tau_s/2)-t, \tag{40}$$

Eq. (29) becomes as follows:

$$-\frac{dv}{dt_1} = \frac{A_a}{M_l}\left(p_s-\frac{F_l}{A_a}\right)-\frac{1}{2}\left(\frac{A_a\tau_s}{K_q y_m}\right)^2\frac{A_a}{M_l}\left(\frac{v}{t_1}\right)^2. \tag{41}$$

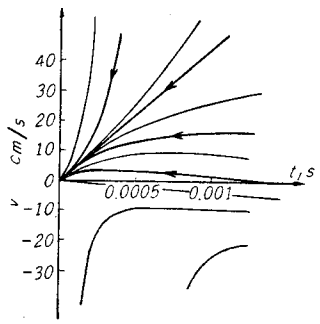

Fig. 8. Velocity of an actuator piston in closing the valve port.

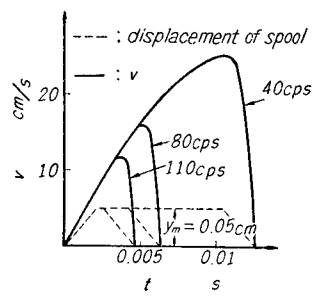

Fig. 9. Velocity of an actuator piston during a half pulse period.

Eq. (41) can be solved by the similar method as with Eq. (30), and the following solution are obtained, corresponding to Eq. (32) and Eq. (34), respectively.

$$v = \frac{a+b}{h}t_1 \quad \text{and} \quad \frac{-(a-b)}{h}t_1, \tag{42}$$

$$v = \frac{t_1}{h}\cdot\frac{(a+b)-(a-b)C_3 t_1^{a/b}}{1+C_3 t_1^{a/b}}. \tag{43}$$

C_3 is determined by the initial condition of $v=v_{10}$ at $t_1=t_{10}$.

$$C_3 = \left[t_1^{-a/b}\left\{\frac{(a+b)t_1-hv}{(a-b)t_1+hv}\right\}\right]_{t_1=t_{10},\, v=v_{10}}. \tag{44}$$

Eqs. (42) and (43) represent a group of curves shown in Fig. 8. When the valve port is closing, three types of curves corresponding to different initial conditions have the physical meaning, as shown by thick lines in Fig. 8.

When the spool is driven in the waveshapes of a trapezoidal pulse, the speed of the actuator piston is represented by the connection of curves obtained from Eqs. (32), (37) and (43). The integration of the connected curves during a half pulse

period gives double-amplitude of the dither, $2u_m$. When τ_s is much smaller than $(T_0/2)$, the trapezoidal pulse is approximated by a rectangular pulse, and double-amplitude of the dither is obtained from Eq. (39) by substituting $t+C_2=(T_0/2)$. Fig. 9 shows the velocity of the actuator piston during a half pulse period for various pulse repetition rate together with the spool displacement, when $y_m=0.05$ cm and $M_l=0.0102\ \mathrm{kg\cdot s^2\cdot cm^{-1}}$.

7. Determination of Pulse Period

In the PWM mode operation, the spool oscillates unceasingly as shown in Fig. 5 (d), and the pulse widths are modulated by the input signals. When a half pulse period, $T_0/2$, approaches to t_D, the waveshape of the spool displacement approaches to triangular pulses. When $T_0/2$ is smaller than t_D, the actuator piston stays no longer at a fixed position even when there is no input signals. The dotted curve in Fig. 10 shows the relation between T_0 and y_m when t_D/T_0 has a constant value. In determining the pulse period, the range over the curve for a fixed value of t_D/T_0 should be used.

The dither amplitude should be small so as not to disturb the output of the servo system. The solid curve in Fig. 10 shows the relation between T_0 and y_m when u_m is constant. In determining the pulse period, the range below the curve for a fixed value of u_m should be used.

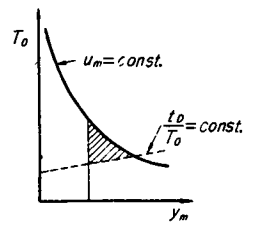

Fig. 10. Diagram for determinig the pulse period.

Moreover, y_m should be so large that the dither velocity and the maximum velocity of the servo output may be sufficiently large. Thus, the pulse period and the maximum displacement of the spool should be selected from the shaded area in Fig. 10.

8. Experiment

The dimensions of the experimental apparatus are as follows:

$x_m=0.35$ mm, $y_m=0.3$ mm and 0.5 mm, $z_m=0.55$ mm, $l_1=22$ mm, $l_2=18$ mm, $I_f=6.78\times10^{-6}\ \mathrm{kg\cdot cm\cdot s^2}$, $p_s=30\ \mathrm{kg\cdot cm^{-2}}$, $A_0=0.785\ \mathrm{mm^2}$, $A_n=3.14\ \mathrm{mm^2}$, $d_n=2$ mm, $A_v=1.767\ \mathrm{cm^2}$, $A_a=1.374\ \mathrm{cm^2}$, $i_1^2n^2K_m=4.44\times10^{-4}\ \mathrm{cm^2\cdot kg}$, $K_q=200\ \mathrm{cm^3\cdot s^{-1}kg^{-1/2}}$, $M_l=0.0102\ \mathrm{kg\cdot s^2\cdot cm^{-1}}$, $F_l=0$.

The following results are obtained by using above dimensions:

$$t_{D_1}=1.85\times10^{-3}\ \mathrm{s},\quad t_{D_2}=2.42\times10^{-3}\ \mathrm{s}.$$

When $y_m=0.3$ mm, $\tau_s=2.64\times10^{-3}$ s and $t_{D_0}=3.46\times10^{-3}$ s. When $y_m=0.5$ mm, $\tau_s=4.40\times10^{-3}$ s and $t_{D_0}=4.34\times10^{-3}$ s.

The output displacement and the current in coils were recorded on oscillogram. Time lag t_{D_0} was considered to be the time required for the actuator piston to reverse the direction of motion after switching the current in a torquemotor. t_{D_0} was measured as follows:

$$t_{D_0} = 5 \times 10^{-3}\,\mathrm{s} \quad \text{when} \quad y_m = 0.3\,\mathrm{mm},$$
$$t_{D_0} = 8 \times 10^{-3}\,\mathrm{s} \quad \text{when} \quad y_m = 0.5\,\mathrm{mm}.$$

Fig. 11 and Fig. 12 show the dither amplitude obtained from the experimental results for $y_m = 0.3$ mm and $y_m = 0.5$ mm, respectively. The analytical results are also drawn by curves in the same figures.

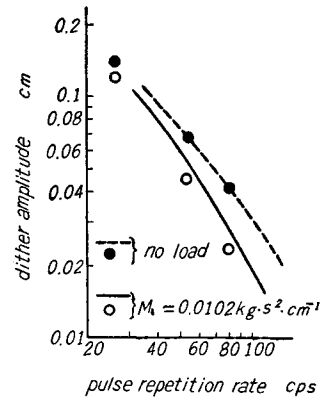

Fig. 11. Dither amplitude for $y_m = 0.3$ mm.

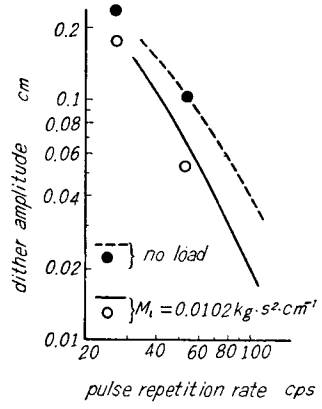

Fig. 12. Dither amplitude for $y_m = 0.5$ mm.

9. Conclusion

The fundamental analysis was performed for a PWM mode electrohydraulic servomechanism composed of a torquemotor, a flapper-nozzle, a spool valve and and an actuator. It was shown that the flapper-nozzle mechanism has a favorable characteristics as the preamplifier of the PWM mode operation. Next, the motions of the flapper, the spool and the actuator piston are analyzed. When the rectangular pulse current is given to two coils of the torquemotor, the spool is driven in the waveshape of trapezoidal pulse by the flapper-nozzle mechanism. When the load of the actuator consists of a mass and friction, the output displacement of the actuator is obtained exactly for the trapezoidal pulse input to the spool valve. The pulse period and the maximum displacement of the spool should be selected from the shaded area in Fig. 10. The analytical results was verified by experiments.

Acknowledgement

The authors would like to express their appreciations to Prof. Y. SAWARAGI for his kind help in carrying out this research.

Nomenclature

x : displacement of a flapper on the central axis of nozzles. [cm]
y : displacement of a spool. [cm]
u : displacement of an actuator piston. [cm]
v : velocity of an actuator piston. [$cm \cdot s^{-1}$]
x_m : clearance between a flapper and a nozzle at the neutral position. [cm]
y_m : clearance between a spool and a stopper at the neutral position. [cm]
z_m : clearance between a flapper and a coil core at the neutral position. [cm]
u_m : dither amplitude of an actuator piston. [cm]
t : time. [s]
Q_{01} and Q_{02}: flow rate through Orifice 1 and 2, respectively. [$cm^3 \cdot s^{-1}$]
Q_{n1} and Q_{n2}: flow rate through Nozzle 1 and 2, respectively. [$cm^3 \cdot s^{-1}$]
α_0, α_n and α_f: discharge coefficient of an orifice, a nozzle and a gap between a flapper and a nozzle, respectively [—]
A_0 and A_n: area of an orifice and a nozzle, respectively. [cm^2]
d_n : diameter of a nozzle. [cm]
A_v and A_a: effective area of a spool and an actuator piston, respectively. [cm^2]
I_f : moment of inertia of a flapper. [$kg \cdot cm \cdot s^2$]
l_1 and l_2: distance as shown in Fig. 1. [cm]
K_m: coefficient for a torquemotor coil. [$cm^2 \cdot kg \cdot amp^{-2}$]
i_1 : current in a coil. [amp]
n : number of turns of a coil [—]
ρ : density of oil. [$kg \cdot s^2 \cdot cm^{-4}$]
p_s : supply pressure. [$kg \cdot cm^{-2}$]
p_{01} and p_{02}: back pressure of Nozzle 1 and 2, respectively. [$kg \cdot cm^{-2}$]
p_{n1} and p_{n2}: downstream pressure of Nozzle 1 and 2, respectively. [$kg \cdot cm^{-2}$]
f_{n1} and f_{n2}: hydraulic flow force of Nozzle 1 and 2 acting on the flapper, respectively. [kg]
t_{D1} : time required for a flapper to arrive at the neutral position after the switching of a torquemotor circuit. [s]
t_{D2} : time required for a flapper to arrive at the opposite nozzle after the switching of a torquemotor circuit. [s]
t_{D0} : time required for a spool to arrive at the neutral position after the switching of a torquemotor circuit. [s]

t_D : time required for a spool to arrive at the opposite stopper after the switching of a torquemotor circuit. [s]

K_q : coefficient of a spool valve. [$cm^3 \cdot s^{-1} \cdot kg^{-1/2}$]

M_l : mass of a load. [$kg \cdot s^2 \cdot cm^{-1}$]

F_l : Coulomb friction. [kg]

References

1) J. E. Gibson and F.B. Tuteur; "Control System Components," McGRAW-HILL, p. 389 (1958)
2) S. A. Murtaugh; Trans. ASME, J. Basic Engg., **18**, Series D, 263 (1959)